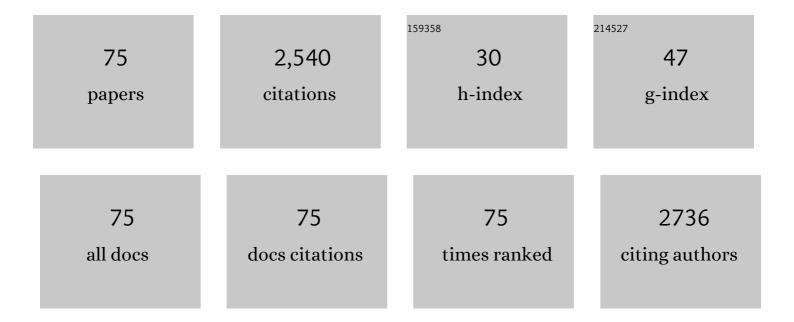
Antonio DurÃ;n Segovia

List of Publications by Year in descending order

Source: https://exaly.com/author-pdf/8008233/publications.pdf

Version: 2024-02-01



#	Article	IF	CITATIONS
1	UV/solar photo-degradation of furaltadone in homogeneous and heterogeneous phases: Intensification with persulfate. Journal of Environmental Management, 2022, 319, 115712.	3.8	1
2	Capture of ambient air CO2 from municipal wastewater mineralization by using an ion-exchange membrane. Science of the Total Environment, 2021, 790, 148136.	3.9	5
3	Effect of reduced graphene oxide load into TiO2 P25 on the generation of reactive oxygen species in a solar photocatalytic reactor. Application to antipyrine degradation. Chemical Engineering Journal, 2020, 380, 122410.	6.6	45
4	Photocatalytic degradation of aniline by solar/TiO2 system in the presence of the electron acceptors Na2S2O8 and H2O2. Separation and Purification Technology, 2020, 238, 116456.	3.9	31
5	Solar photo-degradation of aniline with rGO/TiO2 composites and persulfate. Science of the Total Environment, 2019, 697, 134086.	3.9	25
6	Effect of sodium persulfate as electron acceptor on antipyrine degradation by solar TiO2 or TiO2/rGO photocatalysis. Chemical Engineering Journal, 2019, 364, 257-268.	6.6	97
7	Photocatalytic degradation of aniline using an autonomous rotating drum reactor with both solar and UV-C artificial radiation. Journal of Environmental Management, 2018, 210, 122-130.	3.8	20
8	Study of the intensification of solar photo-Fenton degradation of carbamazepine with ferrioxalate complexes and ultrasound. Journal of Hazardous Materials, 2018, 342, 597-605.	6.5	45
9	Environmental sustainability of the solar photo-Fenton process for wastewater treatment and pharmaceuticals mineralization at semi-industrial scale. Science of the Total Environment, 2018, 612, 605-612.	3.9	84
10	Solar activation of TiO2 intensified with graphene for degradation of Bisphenol-A in water. Solar Energy, 2018, 174, 1035-1043.	2.9	19
11	Sono-activated persulfate oxidation of diclofenac: Degradation, kinetics, pathway and contribution of the different radicals involved. Journal of Hazardous Materials, 2018, 357, 457-465.	6.5	154
12	Operation costs of the solar photo-catalytic degradation of pharmaceuticals in water: A mini-review. Chemosphere, 2018, 211, 482-488.	4.2	48
13	Sono-photo-degradation of carbamazepine in a thin falling film reactor: Operation costs in pilot plant. Ultrasonics Sonochemistry, 2017, 34, 496-503.	3.8	19
14	A novel combined solar pasteurizer/TiO2 continuous-flow reactor for decontamination and disinfection of drinking water. Chemosphere, 2017, 168, 1447-1456.	4.2	24
15	Mineralization of aniline using hydroxyl/sulfate radical-based technology in a waterfall reactor. Chemosphere, 2017, 186, 177-184.	4.2	22
16	Antipyrine removal by TiO 2 photocatalysis based on spinning disc reactor technology. Journal of Environmental Management, 2017, 187, 504-512.	3.8	30
17	Dynamic behavior of hydroxyl radical in sono-photo-Fenton mineralization of synthetic municipal wastewater effluent containing antipyrine. Ultrasonics Sonochemistry, 2017, 35, 185-195.	3.8	27
18	Degradation and mineralization of antipyrine by UV-A LED photo-Fenton reaction intensified by ferrioxalate with addition of persulfate. Separation and Purification Technology, 2017, 172, 227-235.	3.9	58

Antonio DurÃin Segovia

#	Article	IF	CITATIONS
19	Photo-fenton degradation of a beverage industrial effluent: Intensification with persulfate and the study of radicals. Chemical Engineering Journal, 2016, 306, 1203-1211.	6.6	28
20	Modeling the sonophoto-degradation/mineralization of carbamazepine in aqueous solution. Chemical Engineering Journal, 2016, 284, 503-512.	6.6	24
21	Solar photo-degradation of a pharmaceutical wastewater effluent in a semi-industrial autonomous plant. Chemosphere, 2016, 150, 254-257.	4.2	12
22	Application of activated persulfate for removal of intermediates from antipyrine wastewater degradation refractory towards hydroxyl radical. Journal of Hazardous Materials, 2016, 306, 77-86.	6.5	49
23	In situ chemical oxidation of carbamazepine solutions using persulfate simultaneously activated by heat energy, UV light, Fe2+ ions, and H2O2. Applied Catalysis B: Environmental, 2015, 176-177, 120-129.	10.8	227
24	Solar-photo-Fenton treatment of wastewater from the beverage industry: Intensification with ferrioxalate. Chemical Engineering Journal, 2015, 270, 612-620.	6.6	24
25	Solar photodegradation of antipyrine in a synthetic WWTP effluent in a semi-industrial installation. Solar Energy Materials and Solar Cells, 2014, 125, 215-222.	3.0	13
26	Mineralization of wastewater from the pharmaceutical industry containing chloride ions by UV photolysis of H2O2/Fe(II) and ultrasonic irradiation. Journal of Environmental Management, 2014, 141, 61-69.	3.8	25
27	Ultrasound-assisted homogeneous photocatalytic degradation of Reactive Blue 4 in aqueous solution. Applied Catalysis B: Environmental, 2014, 152-153, 59-67.	10.8	47
28	Solar photo-Fenton mineralization of antipyrine in aqueous solution. Journal of Environmental Management, 2013, 130, 64-71.	3.8	16
29	Homogeneous sonophotolysis of food processing industry wastewater: Study of synergistic effects, mineralization and toxicity removal. Ultrasonics Sonochemistry, 2013, 20, 785-791.	3.8	19
30	Sonophotocatalytic mineralization of antipyrine in aqueous solution. Applied Catalysis B: Environmental, 2013, 138-139, 318-325.	10.8	40
31	Optimization of pharmaceutical wastewater treatment byÂsolar/ferrioxalate photo-catalysis. Journal of Environmental Management, 2013, 128, 210-219.	3.8	42
32	Solar photodegradation of synthetic apple juice wastewater: Process optimization and operational cost study. Solar Energy Materials and Solar Cells, 2012, 107, 307-315.	3.0	8
33	Ferrioxalate-induced solar photo-Fenton system for the treatment of winery wastewaters. Chemical Engineering Journal, 2012, 181-182, 281-288.	6.6	47
34	Photocatalytic treatment of an industrial effluent using artificial and solar UV radiation: An operational cost study on a pilot plant scale. Journal of Environmental Management, 2012, 98, 1-4.	3.8	24
35	Optimization of the mineralization of a mixture of phenolic pollutants under a ferrioxalate-induced solar photo-Fenton process. Journal of Hazardous Materials, 2011, 185, 131-139.	6.5	50
36	Roles of different intermediate active species in the mineralization reactions of phenolic pollutants under a UV-A/C photo-Fenton process. Applied Catalysis B: Environmental, 2011, 106, 242-242.	10.8	19

#	Article	IF	CITATIONS
37	Photo-Fenton mineralization of synthetic apple-juice wastewater. Chemical Engineering Journal, 2011, 168, 102-107.	6.6	12
38	Photo-Fenton mineralization of synthetic municipal wastewater effluent containing acetaminophen in a pilot plant. Desalination, 2011, 270, 124-129.	4.0	61
39	Mineralization of integrated gasification combined-cycle power-station wastewater effluent by a photo-fenton process. Journal of Environmental Management, 2010, 91, 1840-1846.	3.8	0
40	Catalytic degradation of Orange II in a ferrioxalate-assisted photo-Fenton process using a combined UV-A/C–solar pilot-plant system. Applied Catalysis B: Environmental, 2010, 95, 120-129.	10.8	54
41	Decontamination of industrial cyanide-containing water in a solar CPC pilot plant. Solar Energy, 2010, 84, 1193-1200.	2.9	18
42	Effect of light source on the catalytic degradation of protocatechuic acid in a ferrioxalate-assisted photo-Fenton process. Applied Catalysis B: Environmental, 2010, 96, 486-495.	10.8	31
43	Photodegradation of Reactive Blue 4 solutions under ferrioxalate-assisted UV/solar photo-Fenton system with continuous addition of H2O2 and air injection. Chemical Engineering Journal, 2010, 162, 702-709.	6.6	47
44	Treatment of IGCC power station effluents by physico-chemical and advanced oxidation processes. Journal of Environmental Management, 2009, 90, 1370-1376.	3.8	10
45	Photocatalytic treatment of IGCC power station effluents in a UV-pilot plant. Journal of Hazardous Materials, 2009, 167, 885-891.	6.5	10
46	Effect of continuous addition of H2O2 and air injection on ferrioxalate-assisted solar photo-Fenton degradation of Orange II. Applied Catalysis B: Environmental, 2009, 89, 510-518.	10.8	61
47	Solar photo-Fenton degradation of Reactive Blue 4 in a CPC reactor. Applied Catalysis B: Environmental, 2008, 80, 42-50.	10.8	46
48	Homogeneus ferrioxalate-assisted solar photo-Fenton degradation of Orange II aqueous solutions. Applied Catalysis B: Environmental, 2008, 83, 46-55.	10.8	90
49	Solar TiO2-assisted photocatalytic degradation of IGCC power station effluents using a Fresnel lens. Chemosphere, 2008, 71, 161-167.	4.2	14
50	Solar photocatalytic degradation of reactive blue 4 using a Fresnel lens. Water Research, 2007, 41, 690-698.	5.3	37
51	Photocatalytic degradation of pollutants from Elcogas IGCC power station effluents. Journal of Hazardous Materials, 2007, 144, 132-139.	6.5	8
52	Fresnel lens to concentrate solar energy for the photocatalytic decoloration and mineralization of orange II in aqueous solution. Chemosphere, 2006, 65, 1242-1248.	4.2	37
53	Scrubbing effect on diesel particulate matter from transesterified waste oils blends. Fuel, 2006, 85, 923-928.	3.4	16
54	Neural networks simulation of photo-Fenton degradation of Reactive Blue 4. Applied Catalysis B: Environmental, 2006, 65, 127-134.	10.8	60

ANTONIO DURÃIN SEGOVIA

#	Article	IF	CITATIONS
55	Treatment of aqueous solutions containing nickel using crandallite-type compounds. Journal of Chemical Technology and Biotechnology, 2006, 81, 262-267.	1.6	6
56	Neural networks estimation of diesel particulate matter composition from transesterified waste oils blends. Fuel, 2005, 84, 2080-2085.	3.4	29
57	Photo-Fenton-assisted ozonation of p-Coumaric acid in aqueous solution. Chemosphere, 2005, 60, 1103-1110.	4.2	36
58	Simulation of diesel particulate matter size. Atmospheric Environment, 2004, 38, 6203-6209.	1.9	7
59	Modelling soot and SOF emissions from a diesel engine. Chemosphere, 2004, 56, 209-225.	4.2	16
60	Elimination of inorganic mercury from waste waters using crandallite-type compounds. Journal of Chemical Technology and Biotechnology, 2003, 78, 399-405.	1.6	11
61	An easy correlation to determine soluble and insoluble fractions in diesel particulate matterâ~†. Fuel, 2003, 82, 2173-2178.	3.4	4
62	Competitive diesel engine emissions of sulphur and nitrogen species. Chemosphere, 2003, 52, 1819-1823.	4.2	4
63	Composition and size of diesel particulate emissions from a commercial European engine tested with present and future fuels. Proceedings of the Institution of Mechanical Engineers, Part D: Journal of Automobile Engineering, 2003, 217, 907-919.	1.1	37
64	Accuracy of the European Standard Method to measure the amount of DPM emitted to the atmosphere. Fuel, 2002, 81, 2053-2060.	3.4	21
65	Simulation of atmospheric PAH emissions from diesel engines. Chemosphere, 2001, 44, 921-924.	4.2	23
66	Assembly of a Thin-Falling-Film Exchanger for Laboratory Demonstrations: Calculation of the Individual Heat-Transfer Coefficient. The Chemical Educator, 2001, 6, 15-20.	0.0	1
67	Improving deactivation behaviour of HZSM-5 catalysts. Applied Catalysis A: General, 2001, 206, 87-93.	2.2	36
68	Modeling diesel particulate emissions with neural networks. Fuel, 2001, 80, 539-548.	3.4	65
69	Development of a suspension copolymerization process for bone cement production. Journal of Applied Polymer Science, 2000, 76, 814-823.	1.3	7
70	The role of sodium montmorillonite on bounded zeolite-type catalysts. Applied Clay Science, 2000, 16, 273-287.	2.6	35
71	Characterization of Soluble Organic Fraction in DPM: Optimization of the Extraction Method. , 1999, ,		21
79	Influence of Mini-tunnel Operating Parameters and Ambient Conditions on Diesel Particulate		20

Measurement and Analysis., 1999,,.

#	Article	IF	CITATIONS
73	Ion-Exchange Calculations Using Spreadsheets. The Chemical Educator, 1999, 4, 231-237.	0.0	1
74	Removal of Acetic Acid by Adsorption from an Ethylene Recycle Stream in the Ethylene–Vinyl Acetate Copolymerization Process. Separation Science and Technology, 1999, 34, 525-543.	1.3	3
75	Degradation kinetics of p-nitrophenol ozonation in water. Water Research, 1992, 26, 9-17.	5.3	77